Available online at www.sciencedirect.com
ScienceDirect
Trans. Nonferrous Met. Soc. China 22(2012) 964−969
Transactions of Nonferrous Metals Society of China
www.tnmsc.cn

Iron reduction in aluminum by electroslag refining

CHEN Chong[1], WANG Jun[1], SHU Da[1], XUE Jing[1], SUN Bao-de[1], XUE Yong-sheng[2], YAN Qing-min[2]

1. State Key Laboratory of Metal Matrix Composites, School of Materials Science and Engineering, Shanghai Jiao Tong University, Shanghai 200240, China;
2. Suzhou Zhenwu Electric Furnace Co., Ltd., Suzhou 215168, China

Received 6 April 2011; accepted 26 July 2011

Abstract: The effect of electroslag refining on iron reduction from commercial aluminum was investigated. Cast electrodes of commercial aluminum were electroslag refined using KCl−NaCl−Na_3AlF_6 slag containing $Na_2B_4O_7$. Experimental results indicate that the iron content decreases with increasing $Na_2B_4O_7$ addition and remelting time, and the iron content decreases from 0.400% to 0.184% under 9% $Na_2B_4O_7$ addition for 30 min remelting. The elastic modulus, yield strength and ultimate tensile strength commercial aluminum are improved, and the tensile elongation is increased by 43% after electroslag refining. The chemical reaction between melt and slag to form Fe_2B is the main reason for iron reduction and the thermodynamic calculation of the chemical reaction theoretically accounts for the formation of Fe_2B.

Key words: aluminum; electroslag refining; iron; mechanical properties; thermodynamic calculation

1 Introduction

Iron is considered the most harmful impurity in aluminum alloys, which comes from the bauxite ore and ferrous metals. Iron has a very low maximum equilibrium solid solubility in aluminum (0.05%, mass fraction) [1], and most iron in aluminum alloys forms together with other alloying elements [2], such as silicon, manganese and copper. Fe-rich intermetallic compounds are responsible for the inferior mechanical properties of aluminum alloys [3,4]. This is mainly due to the precipitation of brittle Fe-rich intermetallic phases which appear as needles or platelets in the microstructure, and these intermetallic phases seriously degrade the tensile strength, elongation and ductility of the alloys [5,6].

The most extensive work on reducing deleterious effect of the brittle Fe-rich intermetallic phases has been carried out for decades. So far, two main categories of methods have been developed. The first is to neutralize the detrimental effect of Fe-rich intermetallic phase by adding chemical elements and thermal treatment [7−10]. Manganese and chromium are the most common alloying addition, which are used to transform the morphology of Fe-rich intermetallic phases from needles or platelets to a more cubic form or globules [7]. Thermal treatments can also modify the morphology and the type of the intermetallic phases [9], but high superheating temperature inevitably leads to high energy costs and high oxidation loss. Furthermore, these treatments can not remove iron from the aluminum alloy and these harmful Fe-rich phases may turn up again in the processing. The second category is the removal of iron from aluminum alloy. Generally, iron removal from aluminum alloy can be carried out by the precipitation and separation of intermetallic phases from the liquid alloys [11−13]. Several techniques, such as filtration, centrifugal and electromagnetic separation, have been developed to separate Fe-rich phases from the liquid alloys. However, it is necessary to add chemical elements to form Fe-rich phases in these processes. The precipitation of Fe-rich phases is greatly influenced by the content of chemical elements and the processing temperature [11]. Moreover, these chemical elements are usually detrimental to the aluminum alloy. Therefore, these methods are very limited in application.

Electroslag refining (ESR) is a secondary refining process which has already been well established for producing steels and other high performance alloys [14−16]. In the process, high current is applied through a

Foundation item: Project (50825401) supported by the National Natural Science Foundation of China; Project (2012CB61905) supported by the National Basic Research Program of China
Corresponding author: WANG Jun; Tel: +86-21-54745387; E-mail: junwang@sjtu.edu.cn
DOI: 10.1016/S1003-6326(11)61271-5

resistive slag layer, and the heat generated within the slag melts a consumable electrode. Metal droplets from the electrode drop through the molten slag and solidify in a mould to form ingot. Refining takes place because of the reaction between the metal and the slag in the process. By suitable choice of slags, chemical reaction between the metal and the slag can be encouraged, such as the removal of impurity elements and retaining necessary alloying elements [14]. STOEPHASIUS et al [16] investigated the removal of the main impurities out of titanium and titanium-aluminum alloys by electroslag refining using a CaF_2-based active slag.

In the present work, electroslag refining was applied to commercial aluminum for the reduction of iron. The effect of electroslag refining on the reduction of iron was systemically investigated, and the thermodynamic mechanism of this process was also discussed.

2 Experimental

Commercial purity aluminum containing 0.40% Fe (mass fraction) was used in the experiment. The composition of the material is listed in Table 1. The slag used was a mixed chloride-fluoride flux, containing 47% KCl, 30% NaCl and 23% Na_3AlF_6 (mass fraction). In addition, the $Na_2B_4O_7$ was added to the slag for the removal of iron and the addition was 3%, 5%, 7% and 9% (mass fraction) of the slag, respectively.

Table 1 Composition of commercial purity aluminum

Fe	Si	Cu	Ga	Mg
0.400	0.040	0.001	0.013	0.002
Zn	Na	K	B	Al
0.002	0.015	0.008	0.004	Bal.

The electroslag remelting experiments were carried out in a 60 kVA single phase AC unit. Figure 1 is the schematic illustration of electroslag remelting unit. Before the electroslag remelting experiments, the commercial aluminum was cast to electrodes with size of *d*40 mm×800 mm and the flux was prefused at 523 K in an oven. In the remelting process, the solid starting technique was used through the arc striking agent. 0.5 kg slag was melted to form the slag bath and the molten slag was super-heated to 1013 K in the remelting process. The electrodes were subjected to electroslag refining to obtain ingots with size of *d*70 mm×(250−300) mm under a voltage of 10−15 V, a current of 600−700 A and a descending speed of 27−107 mm/min. Finally, the sludge was collected for X-ray diffraction (XRD) analysis, and the aluminum samples for metallographic observation and spectrum analysis were taken from the ingots.

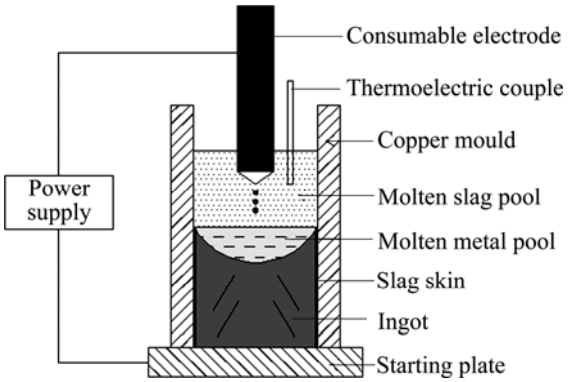

Fig. 1 Schematic illustration of electroslag remelting unit

The chemical compositions of the aluminum sample were analysed with inductively coupled plasma−atomic emission spectrometry machine (ICP-AE3, Iris Advangtage 1000). Metallographs were observed by scanning electron microscopy (SEM, JSM−6460). The original NaCl and KCl in the molten sludge were removed through a deionized water filter process. The phases in the molten slag were detected with an X-ray diffractometer (XRD, D/MAX 2550VL/PC). The tensile properties were tested by a Zwick/Roell test machine. Tensile tests at room temperature were carried out at a tensile speed of 1 mm/min and each value of tensile properties reported was the average of four tests under the same condition. The dimensions of the specimens for mechanical properties testing are shown in Fig. 2.

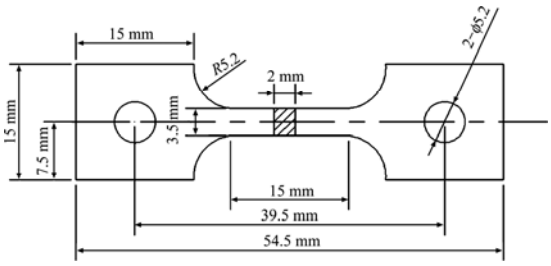

Fig. 2 Dimensions of specimens for mechanical properties testing

3 Results and discussion

3.1 Iron content

Figure 3 shows the dependency of the iron content with different addition of $Na_2B_4O_7$. Regardless of the remelting time, iron content decreases with the increase of $Na_2B_4O_7$ addition. At remelting time of 30 min, the iron content decreases from 0.400% to 0.209% with the addition of 3% $Na_2B_4O_7$. When the addition of $Na_2B_4O_7$ reaches 9%, iron content decreases to 0.184% at the remelting time of 30 min and the maximum iron reduction ratio is 54%. Iron content can be further reduced when the addition of $Na_2B_4O_7$ is more than 9%.

Excessive addition of $Na_2B_4O_7$ should be avoided because it would damage the stability of electroslag refining process. The optimal addition of $Na_2B_4O_7$ is 9%.

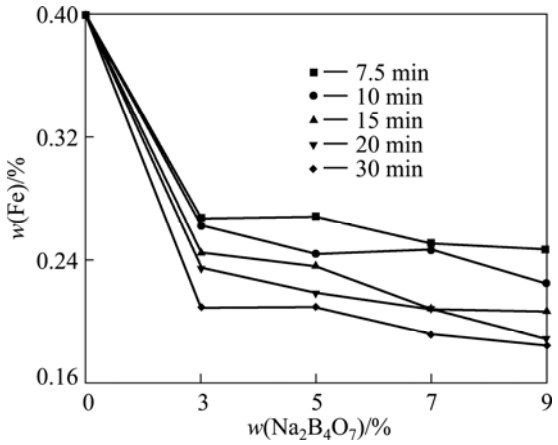

Fig. 3 Iron content with different addition of $Na_2B_4O_7$

Table 2 shows the contents of other impurity elements in the commercial purity aluminum after electroslag refining. Compared with the aluminum sample before electroslag refining, there is no obvious change on the contents of other impurity elements in the aluminum samples after electroslag refining. The result indicates that electroslag refining does not introduce new impurity element to the commercial aluminum after electroslag refining.

The relationship between iron content and remelting time with different $Na_2B_4O_7$ addition is shown in Fig. 4. The iron content decreases as an first order exponential decay function of remelting time with different addition of $Na_2B_4O_7$. The fitted equations corresponding to the curves are also displayed in the figures. With different addition of $Na_2B_4O_7$, iron content decreases rapidly with remelting time and nearly reaches a minimum when the remelting time exceeds 20 min. It indicates that reactions

Table 2 Contents of impurity elements in commercial aluminum with different $Na_2B_4O_7$ addition after ESR

Addition of $Na_2B_4O_7$	Content of impurity elements (mass fraction, %)							
	Si	Cu	Ga	Mg	Zn	K	Na	B
3%	0.039	0.002	0.013	0.002	0.002	0.014	0.007	0.004
5%	0.041	0.001	0.011	0.001	0.001	0.014	0.006	0.003
7%	0.040	0.003	0.012	0.001	0.002	0.015	0.007	0.004
9%	0.038	0.001	0.011	0.002	0.002	0.016	0.008	0.004

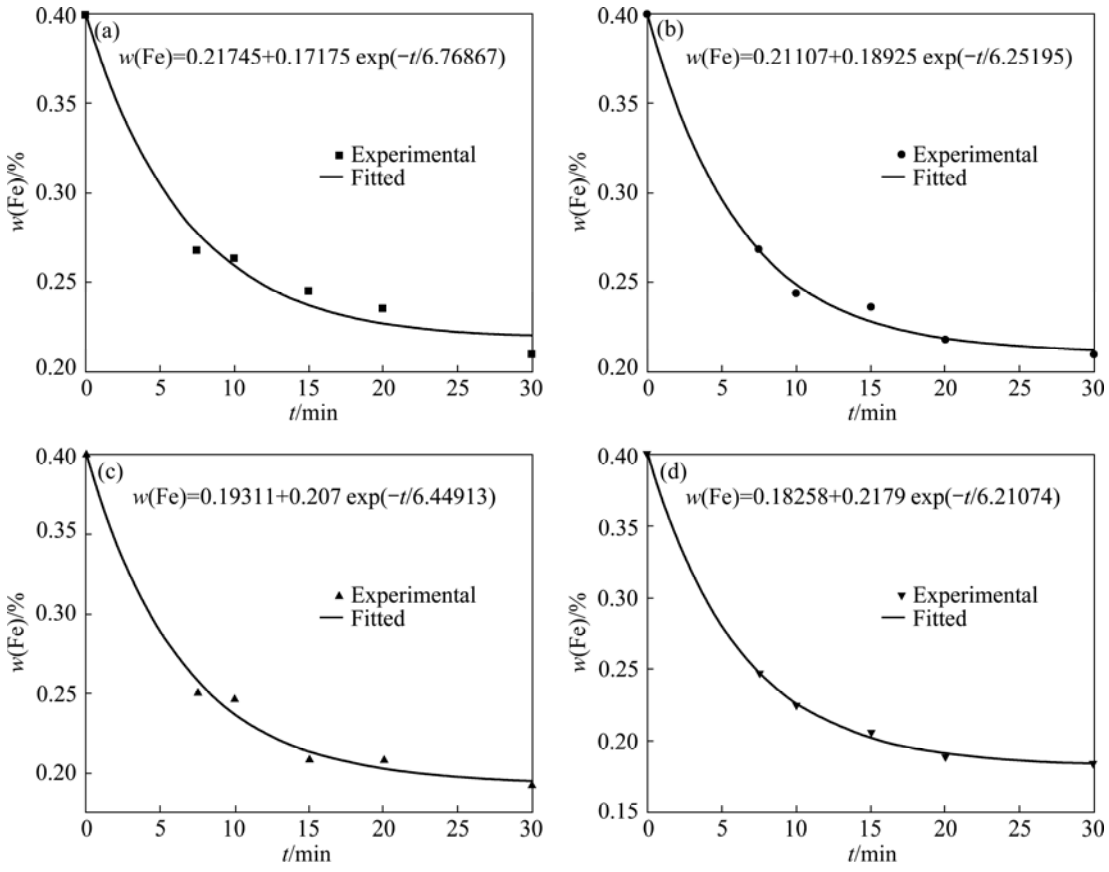

Fig. 4 Relationship between iron content and remelting time with different addition of $Na_2B_4O_7$: (a) 3%; (b) 5%; (c) 7%; (d) 9%

between melt and molten slag has already completed within a period of 20−30 min. Therefore, it is unnecessary to remelt for a longer time, and the optimal remelting time is 30 min.

3.2 Microstructures and mechanical properties

The microstructures of the aluminum samples before and after electroslag refining are shown in Fig. 5. Comparing the micrographs before and after ESR, the needle shaped Al−Fe binary phase at grain boundaries becomes less and thinner obviously.

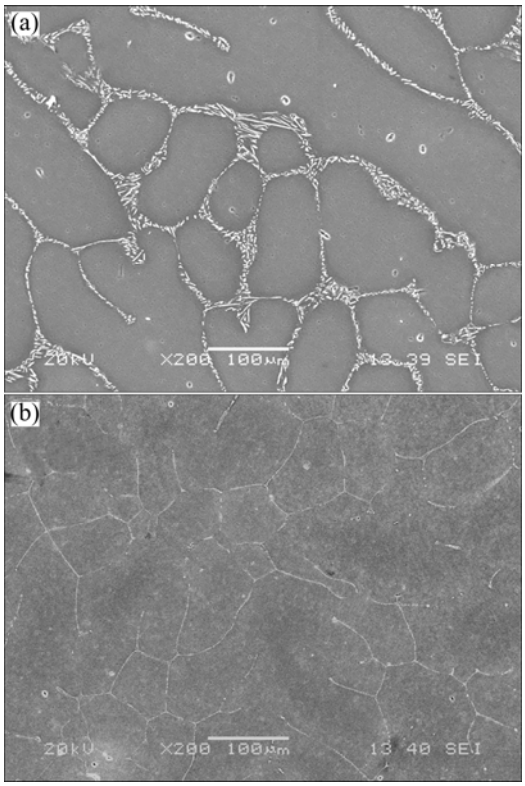

Fig. 5 SEM micrographs of aluminum samples: (a) Before ESR; (b) After ESR with 9% $Na_2B_4O_7$ for 30 min

Figure 6 presents the mechanical properties of the aluminum samples before and after ESR with 9% $Na_2B_4O_7$ addition remelting for 30 min. The result shows that the mechanical properties of the samples after ESR have a minor improvement in the elastic modulus, yield strength and ultimate tensile strength. However, the tensile elongation of the sample after ESR is 43% higher than that of the sample before ESR. The increased tensile elongation and minor improvement in the elastic modulus, yield strength and ultimate tensile strength may be attributed to the reduction of iron [4,5]. After ESR with 9% $Na_2B_4O_7$ addition remelting for 30 min, the Fe content of the aluminum sample decreases from 0.400% to 0.184% and the platelets like Al−Fe binary phase at grain boundaries becomes less and thinner. The probability of cracks initiation on these brittle Fe-rich phases decreases distinctly. Therefore, the mechanical properties of the commercial purity aluminum are improved after electroslag refining.

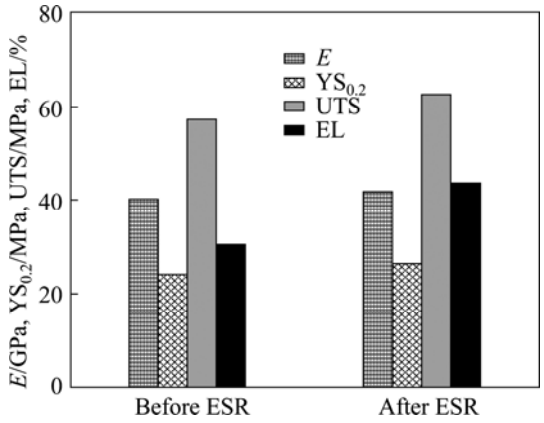

Fig. 6 Mechanical properties of aluminum samples before and after ESR with 9% $Na_2B_4O_7$ remelting for 30 min

3.3 Sludge analysis

The XRD pattern of the collected sludge after electroslag refining is shown in Fig. 7. The elpasolite (K_2NaAlF_6) phase, Al_2O_3 and Fe_2B are found in the sludge. The elpasolite phase is a resultant of AlF_6^{-3} combined with Na^+ and K^+, because Na_3AlF_6, KCl and NaCl are resolved into Na^+, AlF_6^{3-}, K^+ and Cl^- in the molten flux. Al_2O_3 is the common phase in the Al melt, which is captured by molten slag. Fe_2B phase may form as a result of chemical reaction between the iron and $Na_2B_4O_7$ and subsequently be captured by the molten flux during the electroslag refining process. The melting point of Fe_2B is 1389 °C, higher than the temperature of this molten flux [17]. Therefore, the formed particulate Fe_2B can be captured by the molten flux and finally removed with the sludge, which accounts for the fact that the electroslag refining can reduce the Fe content in the commercial purity aluminum.

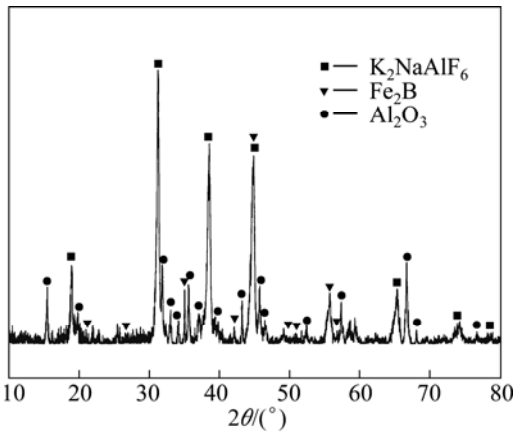

Fig. 7 XRD pattern of collected sludge after electroslag refining

3.4 Thermodynamic calculation

In this chemically complicated slag-melt system, the following reaction may take place to produce Fe_2B among $Na_2B_4O_7$, Fe and Al [18].

$$Na_2B_4O_7(s)+14/3Al(l)+8Fe(l)=7/3Al_2O_3(s)+4Fe_2B(s)+2Na(l) \quad (1)$$

Under practical conditions, the Gibbs free energy of reaction (1) at 1013 K can be calculated as:

$$\Delta G_{1013K}=\Delta G^{\Theta}_{1013K}+RT\ln\frac{a^{7/3}(Al_2O_3)a^4(Fe_2B)a^2(Na)}{a^{14/3}(Al)a^8(Fe)a(Na_2B_4O_7)}$$

$$=\Delta G^{\Theta}_{1013K}+RT\ln\frac{x^2(Na)}{x^{14/3}(Al)x^8(Fe)} \quad (2)$$

where $a(Al_2O_3)$, $a(Fe_2B)$, $a(Na_2B_4O_7)$, $a(Al)$, $a(Fe)$ and $a(Na)$ are the activities of Al_2O_3, Fe_2B, $Na_2B_4O_7$, Al, Fe and Na in the molten droplets, respectively. $a(Al_2O_3)$, $a(Fe_2B)$, and $a(Na_2B_4O_7)$ can be considered to be 1 for solid state matter. For simplification, $a(Al)$, $a(Fe)$ and $a(Na)$ are replaced by their approximately mole fraction: $x(Al)$, $x(Fe)$ and $x(Na)$, respectively. $x(Al)$ and $x(Fe)$ can be calculated as:

$$x(Al)=\frac{0.99542/27}{0.99542/27+0.0040/56}=0.998066 \quad (3)$$

$$x(Fe)=\frac{0.0040/56}{0.99542/27+0.0040/56}=0.001934 \quad (4)$$

In Eqs. (3) and (4), 27 and 56 are the relative atomic mass of Al and Fe, respectively. $x(Na)$ changes with the addition of $Na_2B_4O_7$, as listed in Table 2.

Table 2 Molar fraction of Na with different $Na_2B_4O_7$ additions

Addition of $Na_2B_4O_7$/%	$x(Na)$
3	0.008041
5	0.013402
7	0.018763
9	0.024123

The standard Gibbs free energy at 1013 K, $\Delta G^{\Theta}_{1013K}$, can be calculated by Eq. (5), based on Gibbs free energy function method. Using the standard S_{1013K} and H^{Θ}_{298K} data of the substance shown in Table 3 [19], $\Delta G^{\Theta}_{1013K}$ of reaction (1) can be calculated to be −839614.636 J/mol.

$$\Delta G^{\Theta}_{1013K}=\Delta H^{\Theta}_{298K}-T\Delta S_{1013K} \quad (5)$$

Substituting T with 1013 K, R with 8.314 J/(mol^{-1}·K^{-1}), $x(Al)$ with 0.998066, $x(Fe)$ with 0.001934, $x(Na)$ and $\Delta G^{\Theta}_{1013K}$ with −839614.636 J/mol in Eq. (2), the Gibbs free energy of reaction (1) is calculated under practical conditions, and the results are shown in Table 4.

Table 3 Thermodynamic data of reaction (1)

Substance	S_{1013K} /(J·mol^{-1}·K^{-1})	H^{Θ}_{298K} /(J·mol^{-1})
Al_2O_3	103.136	−1675274
Fe_2B	96.990	−71128
Na	71.182	0
$Na_2B_4O_7$	305.135	−3276490
Al	43.108	0
Fe	42.632	0

Table 4 Gibbs free energy of reaction (1) with different $Na_2B_4O_7$ additions

Addition of $Na_2B_4O_7$/%	ΔG_{1013K}/(J·mol^{-1})
3	−499801
5	−491196
7	−485528
9	−481296

The negative value of ΔG_{1013K} with different $Na_2B_4O_7$ additions indicates that reaction (1) can spontaneously take place in the slag-melt system. The minor difference between the values of ΔG_{1013K} with different $Na_2B_4O_7$ additions also illuminates that the addition of $Na_2B_4O_7$ can hardly affect the occurrence of the reaction. Therefore, thermodynamic calculation theoretically accounts for the formation of Fe_2B in the electroslag refining process.

Moreover, in the electroslag refining process, the reaction takes place in three stages. During the formation of a droplet on the electrode tip, as the detached droplet falls through the slag, and after the molten metal is collected in a pool at the top of the ingot, the reaction interface between melt and slag is multiplied many times. Meanwhile, as the remelting current enters the molten slag in the electroslag refining process, it interacts with its induced magnetism to create the electromagnetic force. The electromagnetic force formed in the electroslag refining process has a function of stirring to the molten slag. Therefore, the reaction balance between melt and slag is broken and the reaction interface is renewed continuously. Therefore, the reaction between melt and slag is improved to great degrees in the electroslag refining process.

4 Conclusions

1) Electroslag refining can decrease the iron concentration in commercial purity aluminum from 0.400% to 0.184% (>54% reduction in iron). The iron content decreases with the addition of $Na_2B_4O_7$ and the remelting time. The optimal addition of $Na_2B_4O_7$ and remelting time are 9% and 30 min, respectively.

2) The elastic modulus, yield strength and ultimate tensile strength of commercial aluminum are improved, and the tensile elongation is increased by 43% after electroslag refining.

3) The chemical reaction between melt and slag to form Fe_2B is the main reason for iron reduction and the thermodynamic calculation theoretically accounts for the formation of Fe_2B spontaneously.

References

[1] ALLEN C M, Q'REILLY K A Q, CANTOR B, EVANS P V. Intermetallic phase selection in 1XXX Al alloys [J]. Progress in Materials Science, 1998, 43(2): 89−170.

[2] MOUSTAFA M A. Effect of iron content on the formation of β-Al5FeSi and porosity in Al−Si eutectic alloys [J]. Journal of Materials Processing Technology, 2009, 209(1): 605−610.

[3] KHALIFA W, SAMUEL F H, GRUZLESKI J E. Iron intermetallic phases in the Al corner of the Al-Si-Fe system [J]. Metallurgical and Materials Transactions A, 2003, 34(3): 807−825.

[4] SHABESTARI S G. The effect of iron and manganese on the formation of intermetallic compounds in aluminum−silicon alloys [J]. Materials Science and Engineering A, 2004, 383(2): 289−298.

[5] MOLLER H, STUMPF W E, PISTORIUS P C. Influence of elevated Fe, Ni and Cr levels on tensile properties of SSM-HPDC Al−Si−Mg alloy F357 [J]. Transactions of Nonferrous Metals Society of China, 2010, 20(s3): s842−s846.

[6] SAMUEL F H, SAMUEL A M, DOTY H W. Factors controlling the type and morphology of Cu–containing phases in 319 Al alloy [J]. AFS Transactions, 1996, 104: 893−901.

[7] de MORAES H L, de OLIVEIRA J R, ESPINOSA D C R, TENORIO J A S. Removal of iron from molten recycled aluminum through intermediate phase filtration [J]. Materials Transactions, 2006, 47(7): 1731−1736.

[8] WANG Y, XIONG Y. Effects of beryllium in Al−Si−Mg−Ti cast alloy [J]. Materials Science and Engineering A, 2000, 280(1): 124−127.

[9] NARAYANAN L A, SAMUEL F H, GRUZLESKI J E. Crystallization behavior of iron-containing intermetallic compounds in 319 aluminum alloy [J]. Metallurgical and Materials Transactions A, 1994, 25(8): 1761−1773.

[10] HOSSEINIFAR M, MALAKHOV D V. Effect of Ce and La on microstructure and properties of a 6××× series type aluminum alloy [J]. Journal of Materials Science, 2008, 43(22): 7157−7164.

[11] FLORES A, SUKIENNIK M, CASTILLEJOS A H, ACOSTA F A, ESCOBEDO J C. A kinetic study on the nucleation and growth of the $Al_8FeMnSi_2$ intermetallic compound for aluminum scrap purification [J]. Intermetallics, 1998, 6(3): 217−227.

[12] CAO X, CAMPBELL J. The solidification characteristics of Fe-rich intermetallics in Al−11.5Si−0.4Mg cast alloys [J]. Metallurgical and Materials Transactions A, 2004, 35(5): 1425−1435.

[13] DAVIGNON G, SERNEELS A, VERLINDEN B, DELAEY L. An isothermal section at 550 °C in the Al-rich corner of the Al−Fe−Mn−Si system [J]. Metallurgical and Materials Transactions A, 1996, 27(11): 3357−3361.

[14] DUCKWORTH W E, HOYLE G. Electro-slag refining [M]. London: Chapman and Hall, 1969: 7−16.

[15] MAITY S K, BALLAL N B, KAWALLA R. Development of ultrahigh strength steel by electroslag refining: effect of inoculation of titanium on the microstructure and mechanical properties [J]. ISIJ International, 2006, 46: 1361−1370.

[16] STOEPHASIUS J C, REITZ J, FRIEDRICH B. ESR refining potential for titanium alloys using a CaF_2-based active slag [J]. Advanced Engineering Materials, 2007, 9(4): 246−252.

[17] YANG C L, LIU F, YANG G C, ZHOU Y Z. Structure evolution upon non-equilibrium solidification of bulk undercooled Fe−B system [J]. Journal of Crystal Growth, 2009, 311(2): 404−412.

[18] GAO J W, SHU D, WANG J, SUN B D. Effects of $Na_2B_4O_7$ on the elimination of iron from aluminum melt [J]. Scripta Materialia, 2007, 57(3): 197−200.

[19] YE Da-lun, HU Jian-hua. Practical handbook of thermodynamic data on inorganic substances [M]. Beijing: Metallurgical Industry Press, 2002: 57−380. (in Chinese)

电渣精炼去除铝中杂质铁

陈 冲[1]，王 俊[1]，疏 达[1]，薛 菁[1]，孙宝德[1]，薛永生[2]，阎庆敏[2]

1. 上海交通大学 材料科学与工程学院 金属基复合材料国家重点实验室，上海 200240；
2. 苏州振吴电炉有限公司，苏州 215168

摘 要：采用添加 $Na_2B_4O_7$ 的 KCl−NaCl−Na_3AlF_6 渣剂对浇注的工业纯铝自耗电极棒进行电渣精炼，以去除纯铝中的杂质铁，并改善其力学性能。结果表明：电渣精炼后纯铝中的铁含量随着 $Na_2B_4O_7$ 添加量和电渣重熔时间的增加而减少，在 $Na_2B_4O_7$ 添加量为 9%和重熔时间为 30 min 的情况下，铁含量从 0.400%降低到 0.184%。电渣精炼后，纯铝的弹性模量、屈服强度和抗拉强度得到改善，尤其是其延伸率提高了 43%。铁含量降低的主要原因是电渣重熔过程中熔渣和铝液滴反应生成富铁相 Fe_2B。渣−液体系的反应热力学计算从理论上解释了 Fe_2B 的生成。

关键词：铝；电渣精炼；铁；力学性能；热力学计算

(Edited by FANG Jing-hua)